KAPL-P-000161
(K97042)
CONF-970568--

FORMATION OF TOUGH COMPOSITE JOINTS

M. K. Brun, (R. Grossman)

May 1997

NOTICE

KAPL ATOMIC POWER LABORATORY SCHENECTADY, NEW YORK 10701

Operated for the U. S. Department of Energy
by KAPL, Inc. a Lockheed Martin company

DISCLAIMER

FORMATION OF TOUGH COMPOSITE JOINTS

M.K. Brun

GE Corporate Research and Development

Schenectady, NY 12301

ABSTRACT

Joints which exhibit tough fracture behavior were formed in a composite with a Si/SiC matrix reinforced with Textron SCS-6 fibers with either boron nitride or silicon nitride fiber coatings. In composites with BN coatings fibers were aligned uniaxially, while composites with Si_3N_4-coated fibers had a 0/90° architecture. Lapped joints (joints with overlapping "fingers") were necessary to obtain tough behavior. Geometrical requirements necessary to avoid brittle joint failure have been proposed. Joints with a simple overlap geometry (only a few fingers) would have to be very long in order to prevent brittle failure. Typical failure in these joints is caused by a crack propagating along the interfaces between the joint fingers. Joints of the same overall length, but with geometry changed to be symmetric about the joint centerline and with an extra shear surface exhibited tough fractures accompanied with extensive fiber pullout. The initial matrix cracking of these joints was relatively low because cracks propagated easily through the ends of the "fingers". Joints with an optimized stepped sawtooth geometry produced composite-like failures with the stress/strain curves containing an elastic region followed by a region of rising stress with an increase of strain. Increasing the fiber/matrix interfacial strength from 9 to 25 MPa, by changing the fiber coating, increased matrix cracking and ultimate strength of the composite significantly. The best joints had matrix cracking stress and ultimate strength of 138 and 240 MPa, respectively. Joint failure was preceded by multiple matrix cracking in the entire composite. The high strength of the joints will permit building of structures containing joints with only a minor reduction of design stresses.

FORMATION OF TOUGH COMPOSITE JOINTS

M.K. Brun

GE Corporate Research and Development

Schenectady, NY 12301

INTRODUCTION

The need for structural materials to operate at higher temperatures is continuously increasing. Ceramic materials have good long-term stability at temperatures above the operating range for current alloys. Ceramics, unfortunately, are subject to catastrophic failure because of their low fracture energies. Even relatively small defects can start cracks that can propagate catastrophically through the component. Reinforcing ceramics with strong fibers, however, has been shown to increase their fracture energy substantially (1,2,3). The work of fracture of a ceramic matrix composite (CMC) can be more than three orders of magnitude higher than that of the matrix. The increased fracture toughness of CMCs, combined with their high creep resistance, make them promising materials for use as structural components at elevated temperatures.

Structural components may have very complex geometries. Consequently, it may be necessary to fabricate them in several pieces which then would be joined together. Another reason why composite components may need to be joined is for the repair of the components after service. In either instance, it will be necessary to produce joints with mechanical properties similar to those of a CMC, joints that will exhibit graceful failure. There has been a considerable amount of work conducted on the joining of monolithic ceramics. All such joints, of course, were brittle. Brittle joint failure is not acceptable for joining CMCs because joint failure would result in catastrophic failure of the component. There has been no report of successful tough joints in the literature to date. The aim of the present work was to establish criteria that joints need to

satisfy and to demonstrate the formation of joints between CMC components which exhibit tough behavior.

The CMC used for the present study was a composite with silicon/silicon carbide matrix reinforced with Textron SCS-6 (SiC) fibers with boron nitride (BN) or silicon nitride (Si_3N_4) coating. These composites have been shown to exhibit tough behavior (1) and can be readily produced in desired shapes.

1. JOINT GEOMETRY

Fiber pullout is the main mechanism that provides the high energy of fracture of the CMC. For a joint to show tough behavior, therefore, its fracture must be accompanied by fiber pullout. When a typical CMC is subjected to load, it behaves in an elastic manner up to a stress level at which the matrix cracks and the stress/strain curve deviates from linearity. On further loading additional matrix cracks are formed and fiber pullout takes place until composite failure. Matrix cracks propagate roughly perpendicular to the fiber axis. For that reason a simple butt joint, shown in Fig. 1a, would not be adequate for CMC joining because it is not expected to fail in tough manner. All the fibers are severed in the joint plane. A crack propagating along the joint plane would not be bridged by any fibers and the fracture would consequently be brittle.

The geometry of the joint needs to be such that not all of the fibers are severed in the same plane. One possible joint geometry is illustrated in Fig. 2. Each side of the joint is machined in a series of "fingers" which will overlap with "fingers" from the other side. All the fingers are defined by surfaces ground parallel to the tensile direction (shaded) which will be referred to as "parallel" and by surfaces perpendicular to the tensile direction (cross-hatched) which will be referred to as "perpendicular" surfaces in this paper. As the crack traverses the composite during failure along any plane such as a', a'' or a''' in Fig. 2b, it will have to cross some part of the composite in which the fibers are continuous. In plane a', for example, 50% of the reinforcing fibers are still continuous, and one would expect approximately 50% of the composite ultimate strength as the best possible joint strength. In order to achieve that strength the joint needs to satisfy some additional criteria which will be discussed in the following paragraphs.

The overall length of the joint is a very important parameter. Each composite system has a characteristic slip length, the distance over which debonding between the matrix and the fiber takes place around a bridged matrix crack. In

the debonded region the matrix only carries a partial load, the load being transferred through the friction at the fiber/matrix interface. The matrix crack spacing, L_c, in a composite is related to the slip length, L_s (4):

$$L_S < L_C < 2L_S \qquad (1)$$

The matrix crack spacing defines a minimum length of the joint. If the embedded fiber length in the joint is not at least equal to the slip length of the composite, the fibers will pull out with relatively low force, and the strength and toughness of the joint will be compromised. If the crack follows plane a" in Fig. 2b, for example, the length of the joint must exceed twice the slip length or fibers could pull out of either end. The slip length in a composite can be estimated from the relation (4):

$$L_s = \left\{ a^2 \frac{V_m^2}{V_f} \frac{E_m E_f}{E} \frac{3m\gamma_m}{4\tau_s^2} \right\}^{\frac{1}{3}} \qquad (2)$$

where L_S denotes the slip length; E_m, E_f, E are Young's moduli of the matrix, fiber, and composite, respectively; V_m and V_f are matrix and fiber volume fraction, respectively, m is the fiber Weibull modulus, γ_m is the critical matrix crack extension energy and τ_s is the fiber/matrix interfacial shear stress.

In a typical Si/SiC matrix reinforced with SCS-6 fibers the crack spacing is of the order of 2 mm (2), which is in good agreement with the prediction of the above formulas. In practice, joint length should be several times larger than the crack spacing. The length of the initial joints was chosen as 12.5 mm.

Another failure mode of a composite that could produce brittle failure is shear along joint surfaces parallel to the tensile direction such as plane b-b in Fig 2b. These planes must have sufficient area to prevent shear failure. That requirement can be estimated by equating shear and tensile loads:

$$\tau \ (n \ L \ t) = \sigma \ (W \ t) \qquad (3)$$

where τ is the shear stress, σ is the tensile stress applied to the sample, W is the sample width, t is sample thickness, L is the joint length, and n is the number of

shear planes in the joint. In the joint shown in Fig. 2, for example, there are three such planes so $n = 3$. Equation (3) establishes the minimum "aspect ratio" for the joint fingers. Rearranging equation (3) obtains:

$$\frac{W}{L} = n\frac{\tau}{\sigma} \qquad (4)$$

The present composite reinforced with 20 wt. % SCS-6 fibers has shear strength of about 60 MPa kpsi at room temperature (2). One can estimate, for example, that the joint shown in Fig. 2 should have its length roughly equal to the width of the test bar to carry a 200 MPa tensile stress.

Considerable optimization of joint geometry may be necessary for specific application. Joints can either contain few fingers and be very long or have many fingers to keep joint length small. There are practical limits to both approaches. The length of the joint will be limited by the type of structure that is being joined. There is also a practical limit to how narrow the fingers can be made. Because of the machining tolerances there has to be some clearance between the fingers and that volume will not contain any reinforcing fiber. Also, the fibers at the edges of the fingers may be damaged by grinding. Therefore, increasing the number of fingers will decrease the volume fraction of reinforcing fiber in the joint.

In production applications, it would be desirable to have geometries which are easy to fabricate. The approach in the current work was to start with the simplest geometries, and increase the joint complexity until satisfactory properties were obtained.

2. EXPERIMENTAL PROCEDURE

Sample preparation has been described elsewhere(1), so only a brief summary will be given here. Textron SCS-6 fibers were supplied with boron nitride or silicon nitride coatings applied by chemical vapor deposition (CVD) on top of their standard carbon coating. Fibers were wound dry on a drum with 0.254 mm pitch. Fiber arrays were taped in the desired length and cut off the drum. The resulting 2-dimensional fiber arrays were taped on a tape casting bed and a carbonaceous matrix slurry was tape cast over them. This process resulted in a 0.23-.28 mm thick tape containing aligned fibers. Tapes were then sprayed with a solution of binder to promote adhesion, stacked in the desired sequence, and

laminated. A majority of samples contained 6 fiber plies, unidirectionally aligned. Some samples (with Si_3N_4 coatings) were produced with 9-ply, 0/90 fiber architecture. An unreinforced layer of matrix tape was added on both outside surfaces of the preform, followed by a layer of sacrificial fibers. The purpose of the sacrificial fibers was to serve as markers during final sample machining. Stacked fiber arrays were laminated by heating under pressure. Preforms were sufficiently strong to be machined into desired shapes. Machining of green preforms was done dry on a surface grinder using a 0.508 mm wide diamond-tipped blade. Preforms were typically 12.7 mm wide, about 3 mm thick with an overall length of about 150 mm.

The sections to be joined were aligned in a fixture. The section of sample around the joint was first saturated with an organic solvent, and then all joint surfaces were coated with a slurry of carbon powder in a solution of organic binders and solvents. If the sample was not saturated with the solvent prior to joining, solvents from the slurry would wick into the sample causing the slurry to set too quickly and prevent proper assembly of the joint. The mating surfaces of the joint were then pushed together, forcing excess slurry to flow out of the joint. Samples were then dried for approximately 2 hours under an infrared lamp to develop sufficient strength for removal from the fixture. Full polymerization of the binders was obtained by heating at 100 °C overnight in an oven. Most of the excess material around the joint was then removed by light sanding.

Infiltration with silicon was carried out under vacuum in a carbon furnace. After binder burnout samples were heated to 1435 °C (about 20 °C above the silicon melting point) for 10 min in contact with a sufficient amount of liquid silicon to convert all of the carbon to SiC and to fill the remaining preform porosity.

After infiltration, the samples were first visually examined for obvious defects and then ground into tensile bars. In the thickness direction, samples were ground to leave approximately .127 mm of unreinforced matrix material covering the first layer of reinforcing fibers. All the samples were tested in tension, using an Instron 1362 servo-electric machine in displacement control mode. Samples were held by hydraulic grips that were aligned prior to all tests and were loaded at a strain rate of 0.127 mm/min. An extensometer was attached to the narrow faces of the sample to monitor sample strain around the joint. Fracture surfaces and polished cross sections were examined by optical microscopy.

4. RESULTS

As mentioned earlier, initial work was conducted on joints with a simple geometry (few fingers), which will be referred to as generation I joints in the rest of this paper. Minor changes in the geometry of these joints resulted in joints with appreciably better behavior, which will be referred to as generation II joints. Further optimization produced the best joints to date, and they will be referred to as generation III joints.

4.1 Generation I Joints

The initial joint geometries are shown in Fig. 1. Joints shown in Figs. 1b and 1c are the simplest geometries possible for a lapped joint. These joints, however, need to be quite long to satisfy the criterion of equation (3) because of the limited number of shear interfaces. Joints shown in Figs. 1d and 1e are somewhat more complicated, but the two halves of the joint have the same geometry, which would make machining a large number of parts easier. In all of the above joints, the joining surfaces are perpendicular to the wide dimension of the bar. In the joint shown in Fig. 1f, the joint surface is parallel to the wide direction of the bar. The advantage of this geometry is that there is a much larger area available to carry the shear load, thus the joint could be made shorter. The disadvantage is that both central fiber plies could be damaged by grinding so that in the 6-ply samples approximately one-third of the fibers may not be capable of carrying load.

Figs. 3a and 3b are stress/strain curves for the joints shown in Figs. 1b and 1d, respectively. The solid lines represent displacement of the crossheads, while the dashed lines represent displacement measured by the extensometer. The curves are typical of all of the lapped joint geometries shown in Fig. 1. The stress increased linearly to a maximum, ranging from 60 to 90 MPa at which point the joint cracked. Joints retained some load-carrying capability after the initial cracking, however, the stress that they could support generally did not exceed the initial cracking stress. Joints with a larger interfacial area (more "fingers") generally retained higher load-carrying capability after the initial cracking than the joints with simpler geometries.

The displacement measured by the extensometer, shown with dashed curves in Figs. 3a and 3b, was linear up to the initial cracking. After the initial cracking some samples exhibited a sudden increase in strain, which would be expected because of the crack within the joint. In other samples, however, a sudden negative deviation was indicated. Because samples could not contract under

tensile loading the negative strain is an indication of sample bending. Bending could occur if the initial crack formed on one side of the sample, making that side more compliant. If the extensometer is located on the side of the sample opposite the opening crack it would indicate an apparent contraction of the sample.

Visual inspection and examination with an optical microscope indicated that all samples had failed by crack propagation around all the fingers. None of the joints should have failed in shear at such low stress levels, if the stress was distributed uniformly across the joint. Bending of the sample after the initial cracking, however, would cause high local stress at the crack tip which made it possible to propagate the crack along the remaining joint surfaces.

The main observations that were made on the initial joint geometries were: (1) to prevent "unzipping" of the joint there had to be a sufficient number of shear surfaces, (2) joint geometry had to be symmetric about the centerline to prevent sample bending, and (3) the "perpendicular" surfaces intersecting the sample edge should be of minimal length to minimize sample bending after initial cracking.

4.2 Generation II Joints

The joint geometry incorporating improvements based on the results obtained with the original set of joints is shown in Fig. 4a. This joint had four shear surfaces and relatively narrow "perpendicular" surfaces intersecting the sample edges. The center sections were made correspondingly wider, so that approximately 50% of the fibers were severed at each end of the joint. The fracture characteristics of these joints differed significantly from those shown in Fig. 1. There were no failures caused by crack propagation along the joint interfaces. A typical stress/strain curve for this type of joint is shown in Fig. 5. Stress increased linearly up to about 50 MPa where a crack formed at one end of the joint. A minor stress decrease at that point was followed by a further stress increase. Typically, a second crack developed at the other end of the joint, indicated by another drop in stress level, and then extensive fiber pullout took place.

The strain-to-failure of these joints was very long (in excess of 1%), as indicated by the extensometer reading. Strain measured by the extensometer was larger than the strain calculated from the displacement of the crossheads. The reason is that crosshead strain is averaged over the entire sample length, while deformation was largely limited to joint area. There was no indication of

sample bending during fracture. A macro photograph of a failed joint is shown in Fig. 6 showing that extensive fiber pullout had taken place.

The initial matrix cracking stress in these joints was low when compared to the cracking stress in CMC without a joint. The main reason that cracking occurred at such low load is that all of the "perpendicular" surfaces are aligned at the ends of the joint, which provides an easy path for a crack to follow. A geometry that attempted to improve initial cracking stress is shown in Fig. 4b. The potential advantage of this type of joint is that there are fewer "perpendicular" surfaces in any given cross section of the joint. Also, only approximately one-third of the fibers were severed at each of the three planes. The disadvantage, of course, was that the joint had to be twice as long as the one in Fig. 4a to carry the same shear loading. There was, however, only a marginal improvement of either matrix cracking stress or of the ultimate stress when compared to the joint shown in Fig. 4a. Since it was desirable to keep the total length of the joints as short as possible, the geometry shown in Fig. 4a was considered preferable.

The photomicrograph in Fig. 7 shows a cross-section through a fairly typical joint. Adjacent fingers are identified by the presence of the fibers. The area between the fingers contains a large, light colored area which represents a region that contains only silicon. Absence of SiC indicates that prior to infiltration the region was either a pore or a pool of binder without any carbon powder. These regions were formed during the assembly of the joint. Typically, joints were assembled by placing the two pieces into the alignment grooves in the fixture and sliding them toward each other until the surfaces were mated. Due to the relatively long sliding distances, there is a possibility that the slip would be scraped from the mating surfaces and would be pushed toward the joint ends, leaving the space between the fingers largely devoid of material. To minimize this problem, attempts were made to assemble joints by aligning the two mating surfaces above each other and then sliding them together vertically so that the maximum sliding distance would be equal to the thickness of the sample. These attempts were not always successful, and the space between the original joint parts contained a high volume fraction of silicon.

4.3 Generation III Joints

The joint geometry that addresses both concerns - not having a plane for easy crack propagation, and enabling good filling of the joint with slip is shown in Figs. 8a and 8b. These are variations of the sawtooth type geometry with an included angle of about 14 and 10 degrees, respectively. The angle had to be small enough to have a sufficient surface area to carry shear loads. The overall

length of the joints shown in Fig. 8a and 8b was 15.2 and 19 mm, respectively. The step-like geometry was used to simulate smooth sawtooth geometry because of the ease of grinding. Smooth sawtooth geometry would require reproducible tilting of the specimen in the grinding machine which would be difficult to achieve. The stepped geometry, on the other hand, can be easily ground on a numerically controlled (NC) grinding machine without moving the sample. The main advantage of this geometry, as already mentioned, is that there are no distinct large "perpendicular" surfaces to provide an easy path for the initial crack. A second advantage is that the joint could be filled reliably with the joining slip.

Figure 9 is the stress/strain curve obtained for the joint shown in Fig. 8a. The initial matrix cracking stress was at 105 MPa, followed by extensive fiber pullout and continued increase in stress-carrying capability. Ultimate stress and strain were 145 MPa and 1.5%, respectively. Joints of this type exhibited desired tough behavior, however, the ultimate strengths were considerably lower than the ultimate strength for the same composite without a joint (up to 525 MPa).

Samples exhibited a very high degree of fiber pullout during failure. In most cases the entire length of fiber that was embedded in the joint pulled out. One such fractured joint is shown in Fig. 10. The triangular shaped regions contain no matrix, only fibers. None of the fibers that were embedded within the joint failed. The fibers which pull out of the matrix completely do not carry the maximum load that they are capable of carrying. In order to get maximum joint strength, fibers within the joint need to be loaded to their failure stress.

4.4 The effect of fiber/matrix interfacial strength

The load transfer between fiber and matrix takes place through shear stress at the interface. The two means by which the load transfer between the fibers and the matrix can be improved are either: (1) by increasing the embedded fiber length or (2) by increasing the fiber/matrix interfacial shear strength. Embedded fiber length would be increased by increasing the joint length which, as discussed earlier, is not a desirable approach.

The fiber/matrix interfacial strength can be tailored by the choice of fiber coating. Present composites with the BN fiber coating have an average interfacial strength of about 8 MPa, as measured by the fiber pushout technique. Replacing the BN fiber coating with Si_3N_4 coating increases the interfacial shear strength to about 35 MPa. Composites with Si_3N_4 coatings were processed in the same manner as the composites with BN coatings, except for the fiber

architecture. While fibers in the composites with the BN coatings were aligned uniaxially, fibers in the Si_3N_4 composites were arranged in a 0/90 layup.

Joints were made with the "optimized" stepped sawtooth geometry, shown in Fig. 8. The stress/strain curve for such joints is shown in Fig. 11. The curve for an identical composite sample not containing a joint is also included for comparison. The joint shows tough fracture behavior: stress increases linearly to about 138 MPa (>90% of unjoined CMC), followed by matrix cracking and continuous stress increase up to failure at about 240 MPa, which represents more than 50% of the strength of unjoined composite. The sample failed in a manner similar to the failure of a composite without a joint, with multiple matrix cracking taking place throughout the stressed region of the bar, both within and outside of the joint. The final failure crack was within a joint; however, it also was largely perpendicular to the tensile direction, as would be expected in an unjoined composite.

The first matrix cracking stress and the ultimate strength of the joints containing Si_3N_4 fiber coating are significantly higher than in the composite with BN coating. Both effects are due to the higher fiber/matrix interfacial shear strength. First matrix cracking is improved because higher shear strength results in more efficient load transfer from the matrix to the fibers, so that they carry a larger fraction of the total load. Equation (1) shows that an increase in the interfacial strength will result in a decrease of the composite slip length. Since the joint length is held constant the ratio of the embedded fiber length to the slip length increases. The ultimate strength of the joint will consequently increase because fibers cannot pull out of the matrix without fiber failure.

The first matrix cracking stress of the joints is only about 5% lower than that of unjoined composite (compare the two curves in Fig. 11). It is generally accepted that the design stress for CMCs will be close to the first matrix cracking stress. Having the matrix cracking stress close to that of the unjoined composite means that the design stresses will not have to be significantly derated due to the presence of the joints. It is also important that the ultimate strength of the joined composite is significantly higher than the composite matrix cracking stress. The high ultimate stress makes it possible to make "safe" designs with joints.

5. SUMMARY

Joints which exhibit tough fracture behavior were formed in a CMC consisting of Si/SiC matrix reinforced with Textron SCS-6 fibers. Lapped joints were required to obtain tough behavior. Geometrical requirements for such joints have been established. The effect of the joint geometry and of the fiber/matrix

interfacial strength on the tensile properties of such joints has been studied. Joints with very simple geometries would have to be very long and symmetric in order to prevent brittle failure caused by cracks propagating along the joint interface. Joints of the same overall length, but with improvements in size and symmetry of fingers had tough fractures accompanied with extensive fiber pullout. The initial matrix cracking stress for these joints was relatively low because cracks propagated easily through the ends of the fingers. However, joints with an optimized stepped sawtooth geometry exhibited composite-like fractures. Increasing the fiber/matrix interfacial strength (by changing the fiber coating) resulted in a dramatic increase in matrix cracking stress and ultimate strength of the joints. The best joints had a first matrix cracking stress of 138 MPa (>90% of the original CMC) and ultimate strength 240 MPa (>50% of the original CMC). Joint failure was preceded by multiple matrix cracking through the entire stressed region of the composite, both within and outside the joint. The high strength of the joints will permit design of structures containing joints with only a minor reduction of the design stresses.

ACKNOWLEDGMENTS

I am grateful to W. A. Morrison for sample preparation and helpful discussions, K.L. Luthra for critical discussions and review of the manuscript and P. Breslin for preparation of the manuscript. This work was supported in part by DOE/CFCC Contract No. DE-FC02-92CE41000, Joe Mavec, contract monitor.

REFERENCES

1. "Toughened Silcomp Composites - Process and Preliminary Properties," K.L. Luthra, R.N. Singh, and M.K. Brun, The American Ceramic Society Bulletin, 72 [7], (1993) pp. 79-85.

2. "SiC Monofilament Reinforced SiC-Si Matrix Composites: I. Preform Processing by Tape Casting and Lamination," M. K. Brun, G. Corman, D. Utah and K. L. Luthra, to be submitted to Journal of The American Ceramic Society

3. "SiC Fiber Reinforced Silcomp (Si-SiC) Composites," K.L. Luthra, R.N. Singh, and M.K. Brun, High Temp. Cer. Matrix Composites, R. Naslain, J. Lamon, and D. Doumeing (Eds.), 6th European Conf. on Comp. Matls., 20-27 Sept. 1993, Bordeaux, France, Woodhead Publishing Ltd., (1993), pp. 429-436.

4. "Single and Multiple Fracture," J. Aveston, G.A. Cooper, A. Kelly, The Properties of Fiber Composites, Conf. Proceedings, National Physical Laboratory, IPC Science and Technology Press Ltd., (1971), pp. 15-26.

LIST OF FIGURES

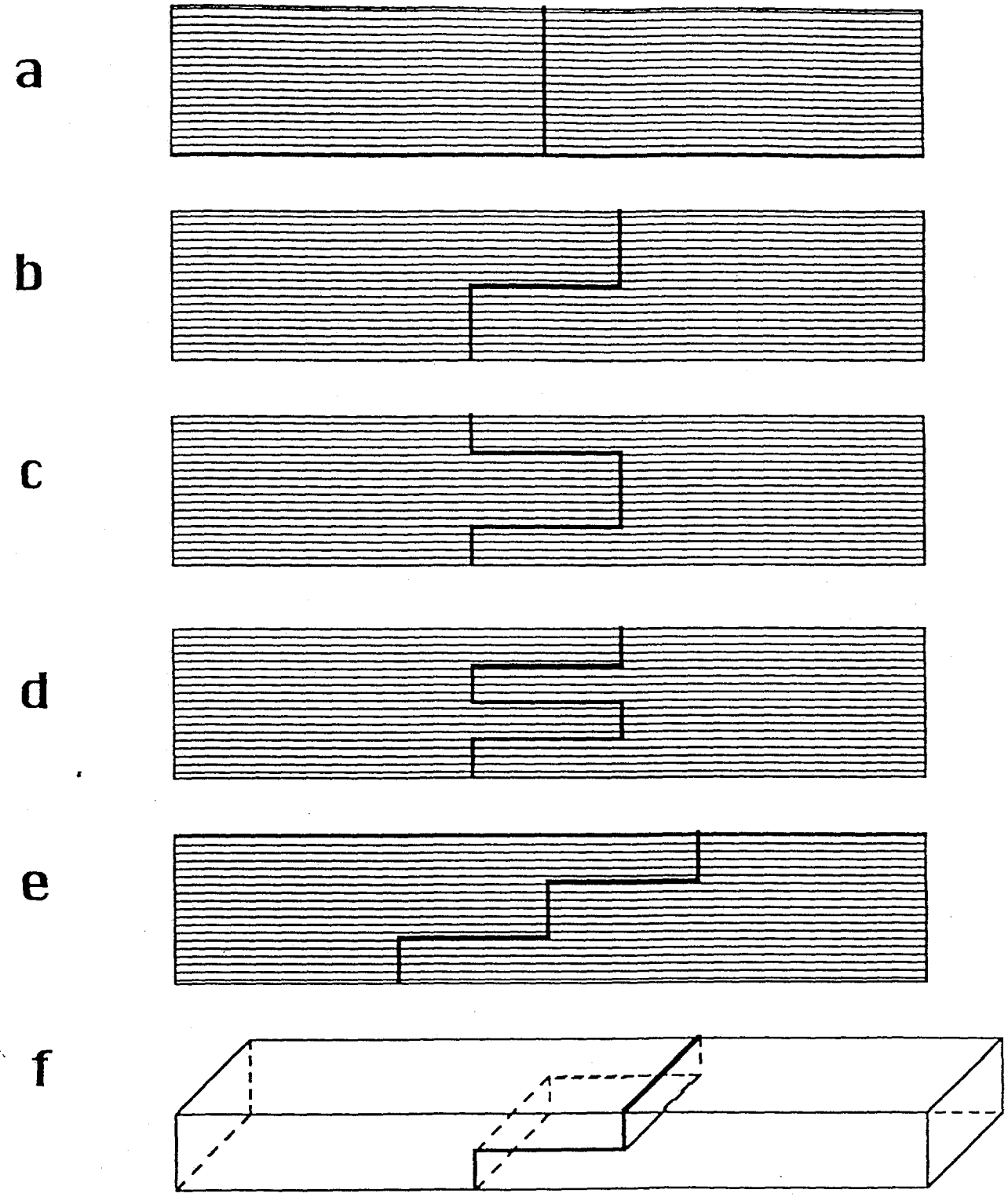

Fig. 1. Geometry of simple joints. Joint 1e is 25.4 mm long, while all other joints are 12.7 mm long

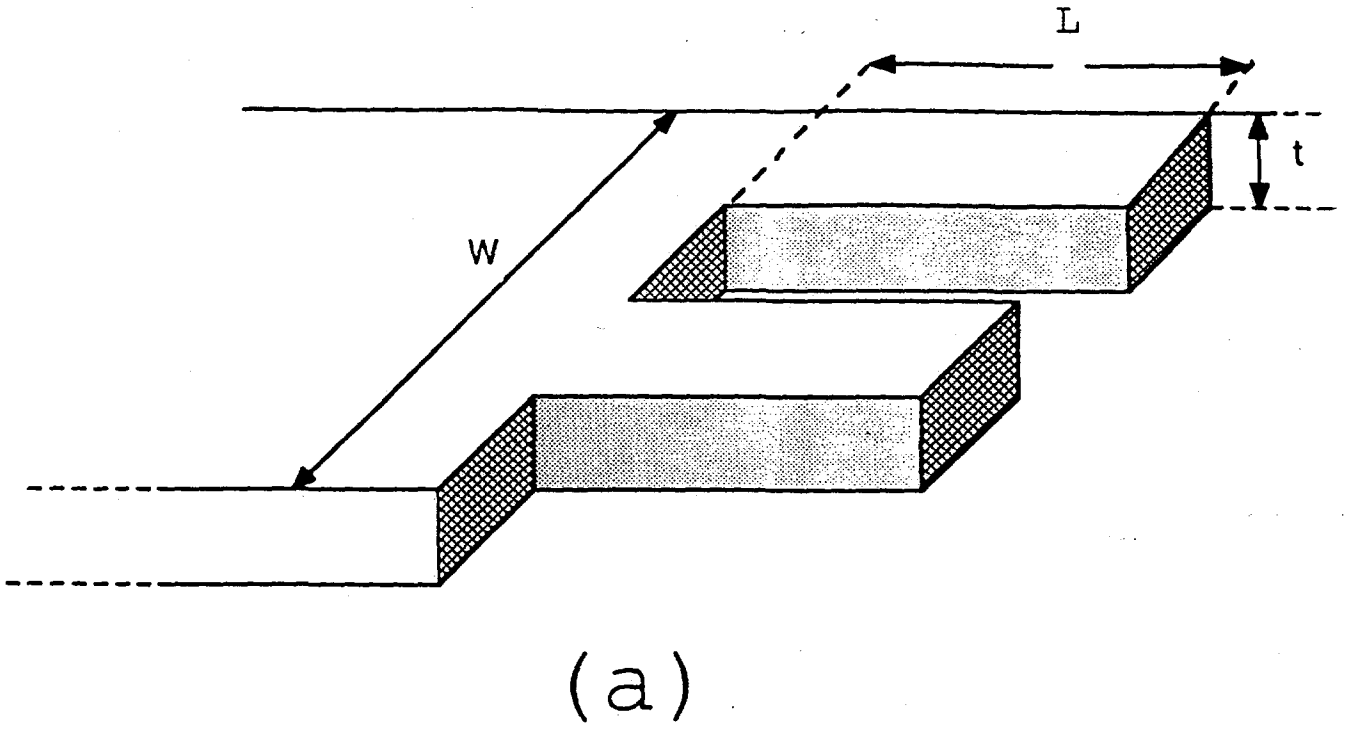

(a)

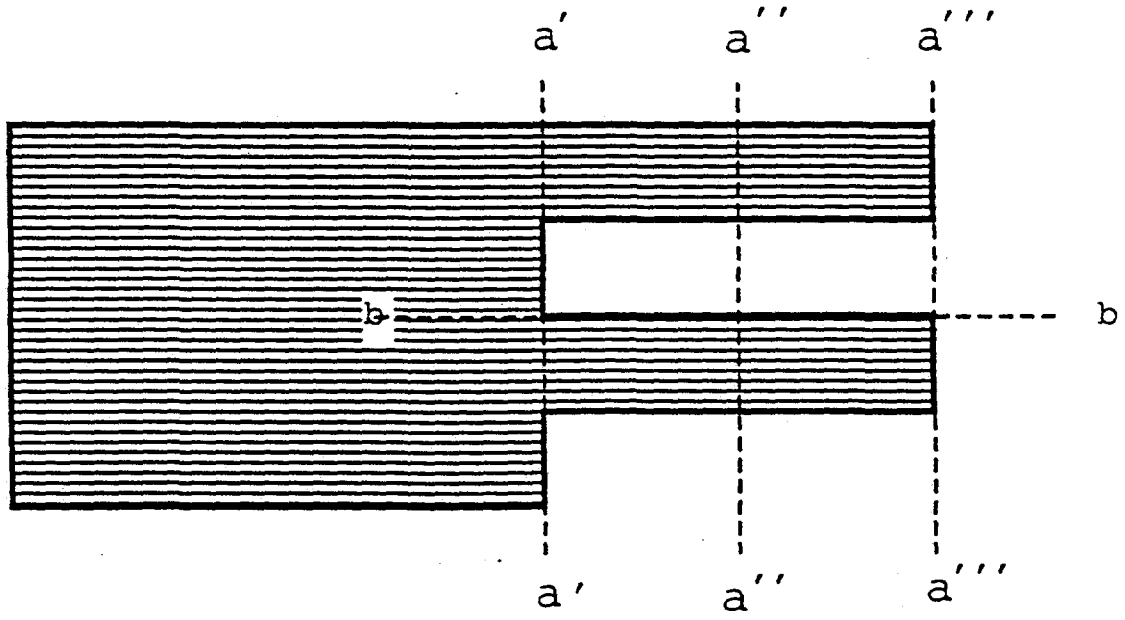

(b)

Fig. 2. An isometric and a top view of a typical lapped joint.
W = width, L = length, t = thickness

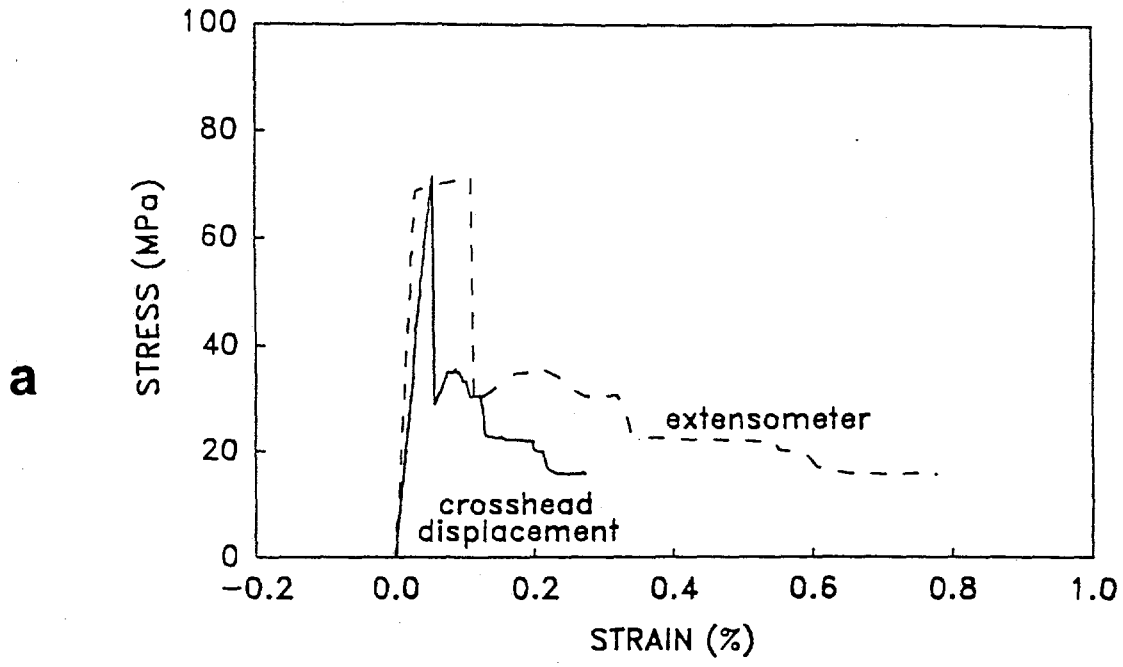

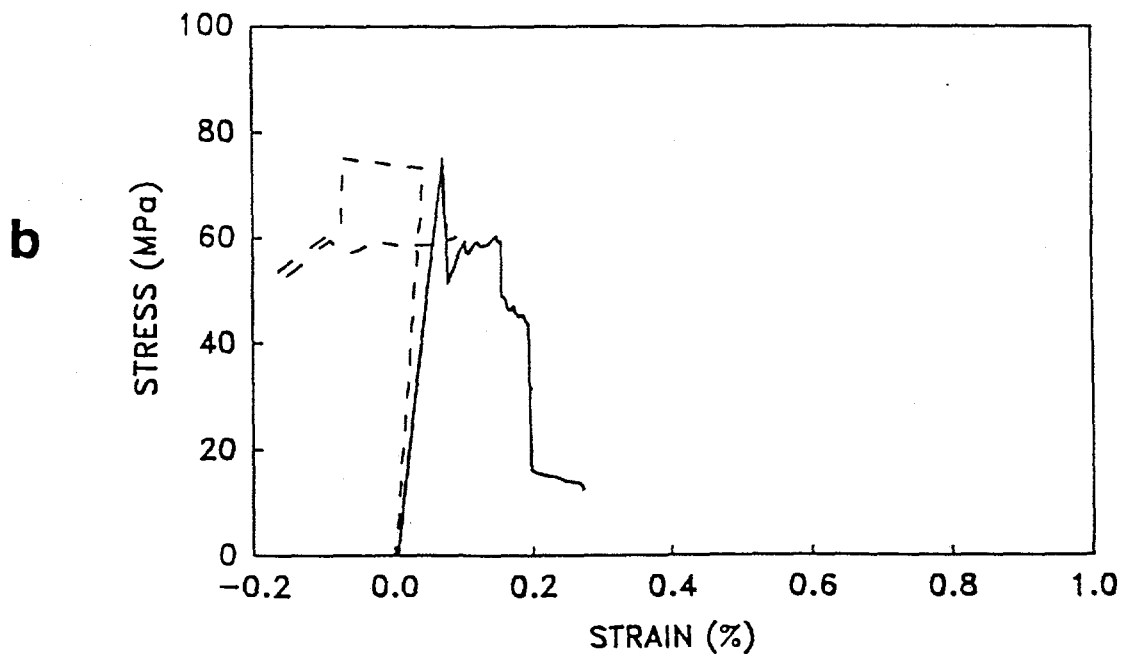

Fig. 3a and 3b. Stress/strain curves for joint geometries shown in Fig. 1b and 1d, respectively. Crosshead displacement is shown as solid lines while displacement measured with the extensometer is shown as dashed lines.

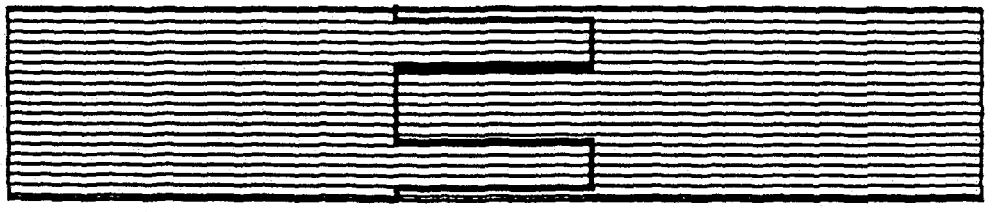

a

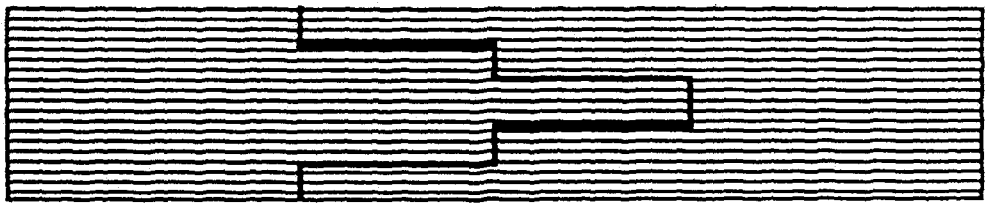

b

Fig. 4. Geometries of the generation II joints.
Joints a and b are 12.7 and 25.4 mm long, respectively.

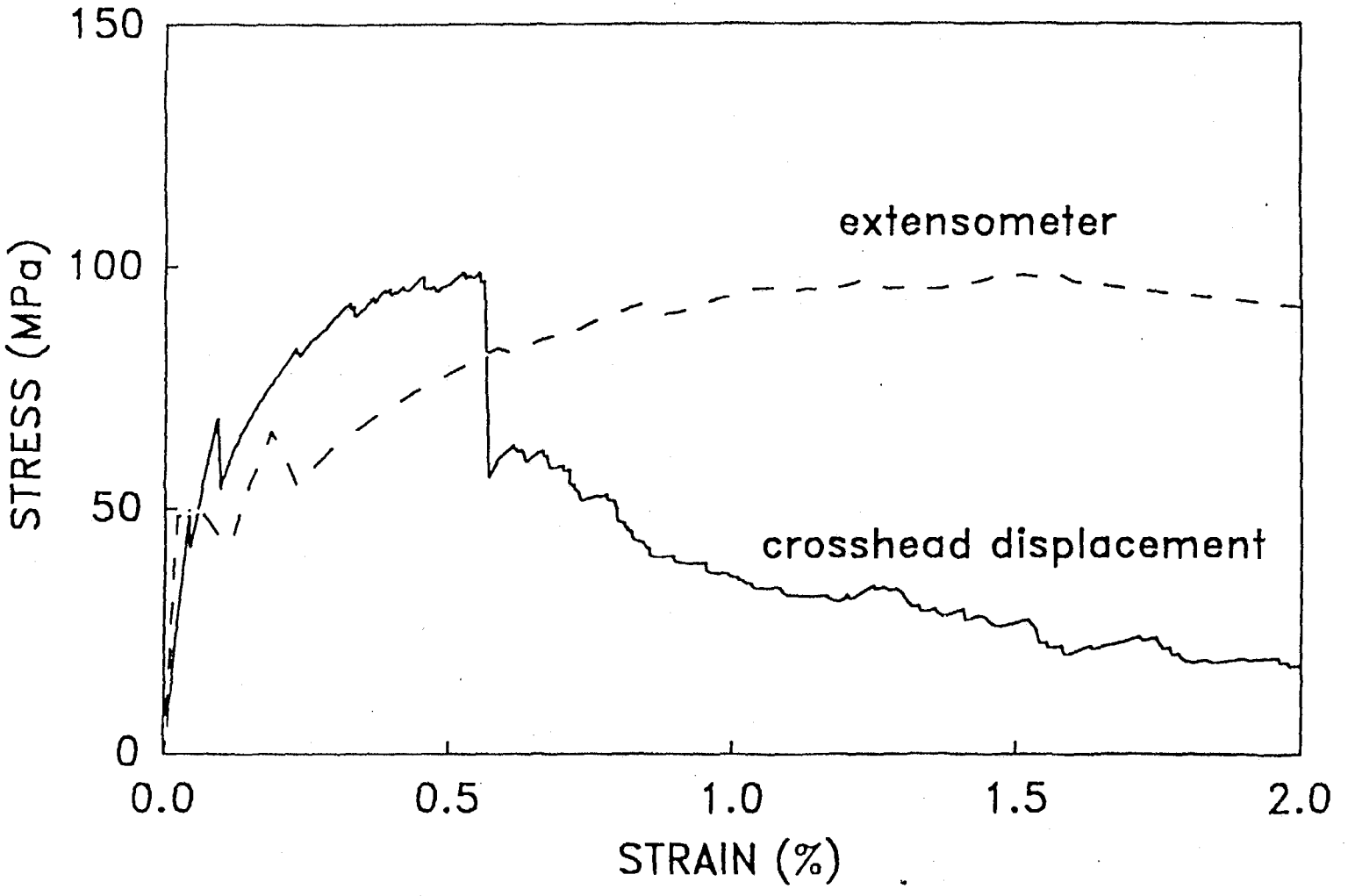

Fig. 5. Stress/Strain curve for the joint shown in Fig. 4a.

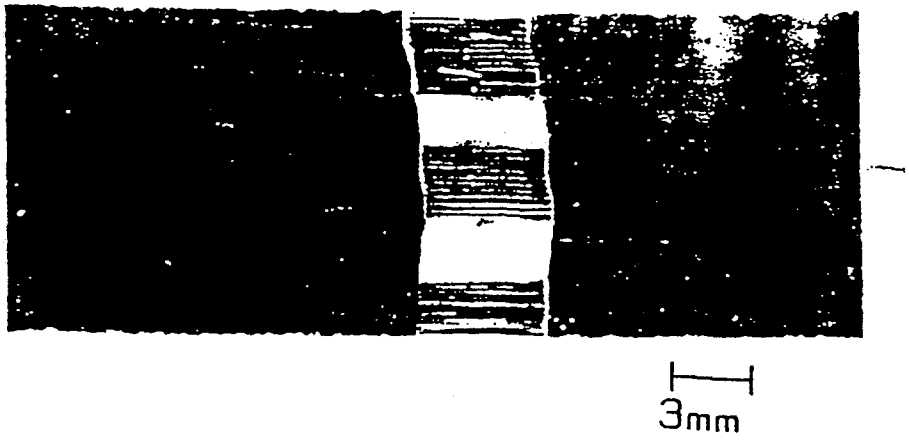

Fig. 6. Macrophotograph of the joint shown in Fig. 4a after testing. Note extensive fiber pullout.

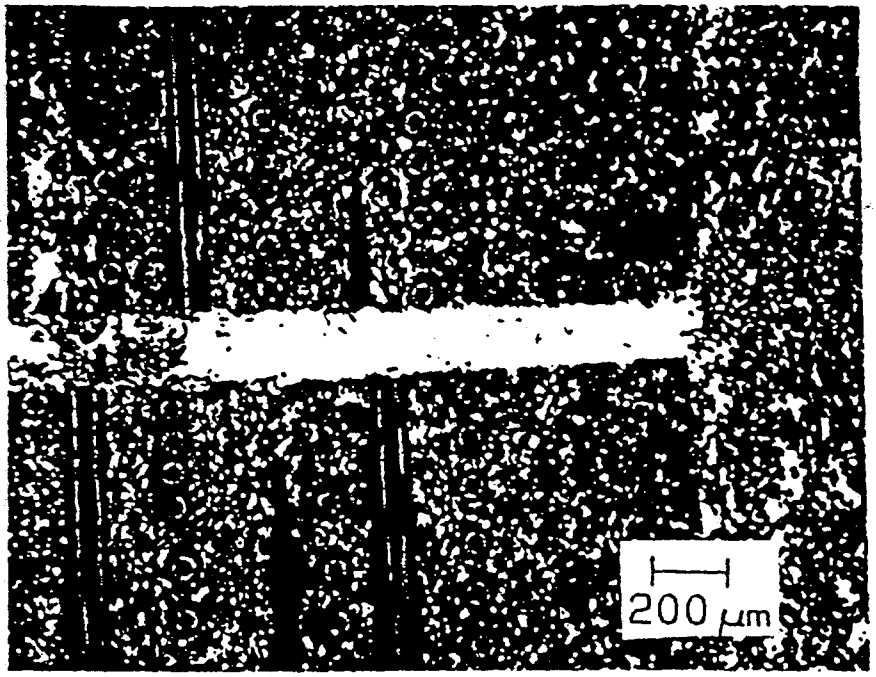

Fig. 7. Photomicrograph of a joint with clearance area between "fingers" (devoid of fibers) only partially filled with joining slip. Bright phase is Si, gray phase SiC and black phase carbon.

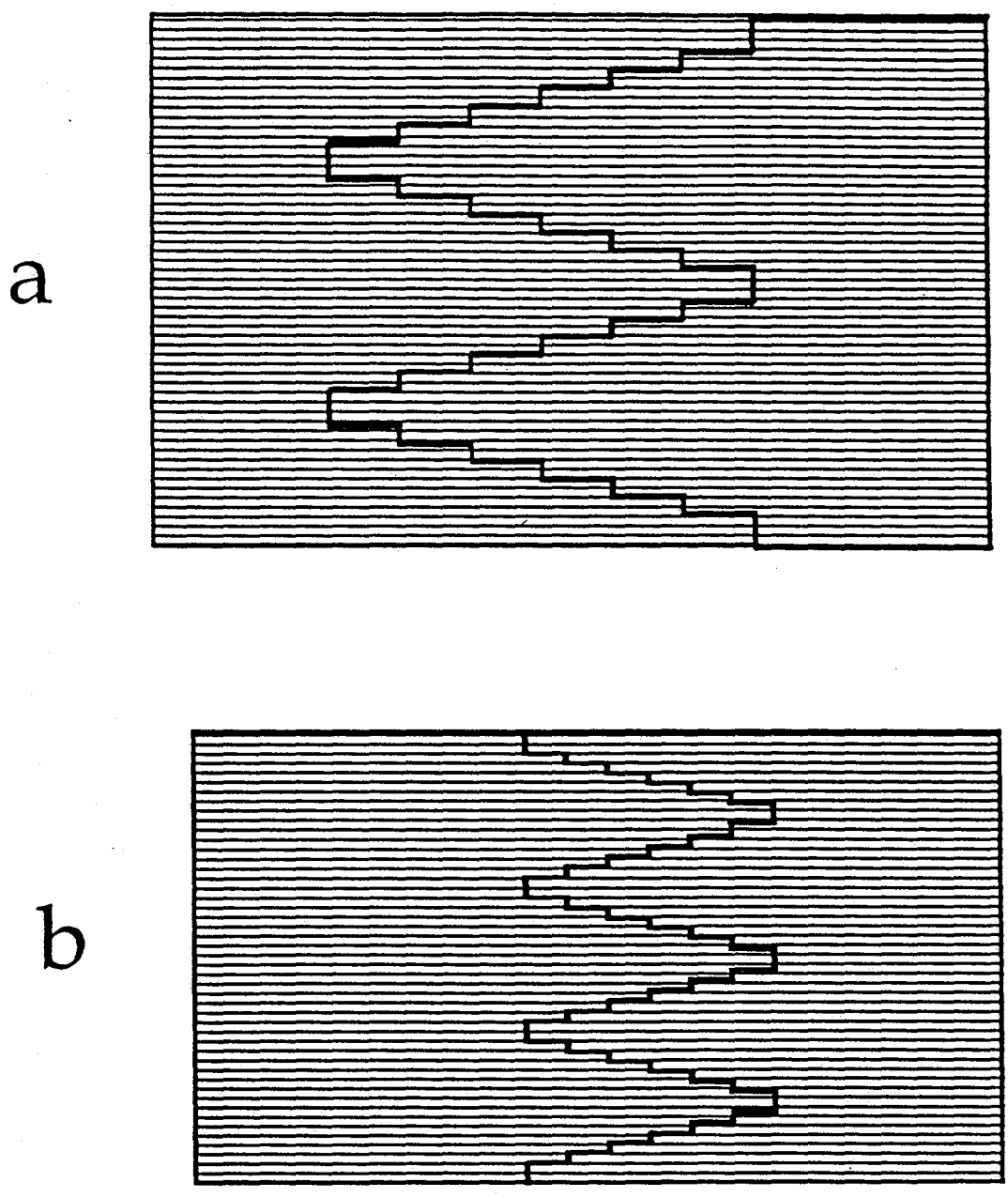

Fig. 8. Geometry of Generation III joints. Joints a. and b. have a 14 and 10 degree included angles and are 15.2 and 19 mm long, respectively.

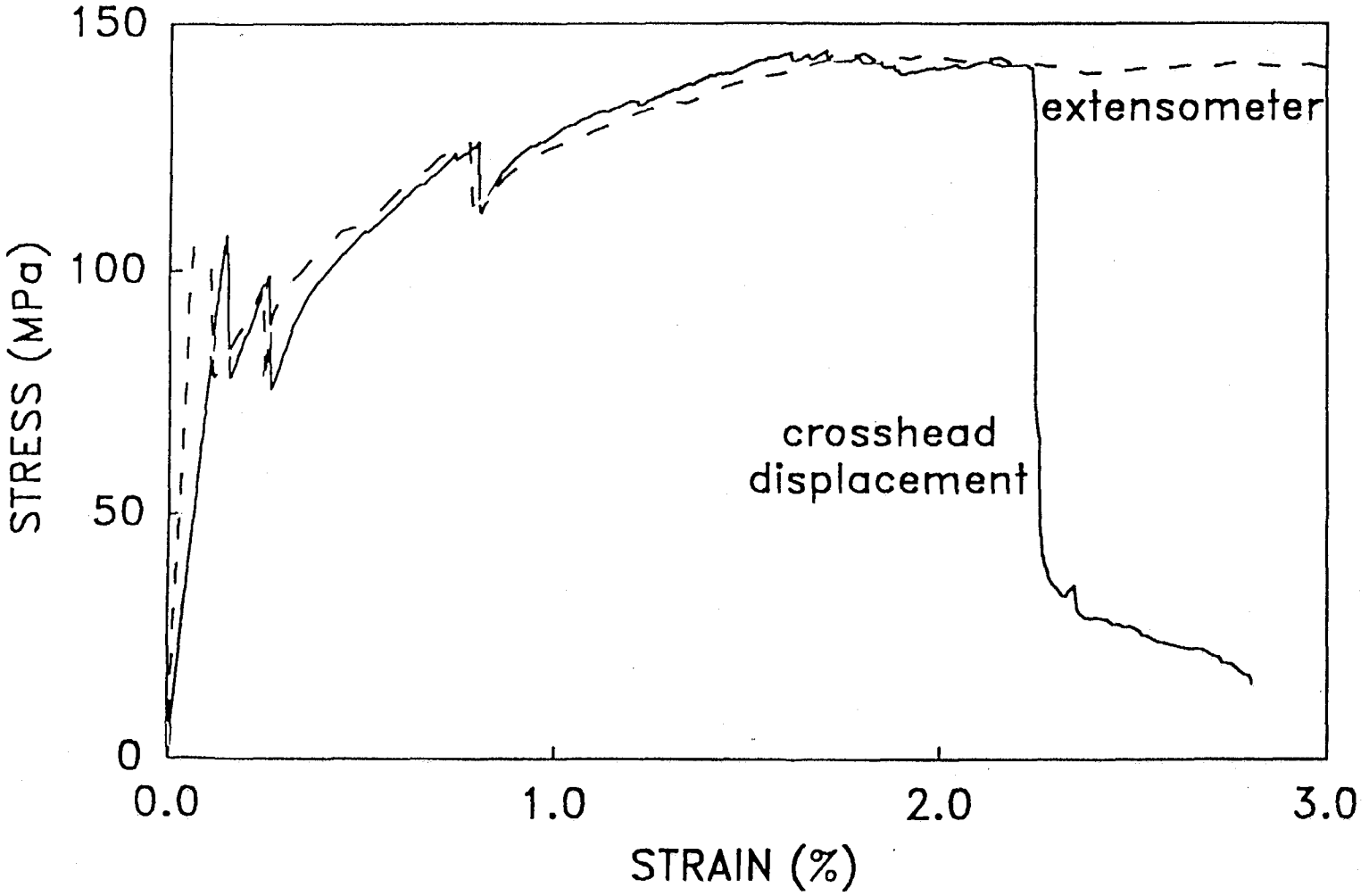

Fig. 9. Stress/Strain curve for the joint shown in Fig. 8a.

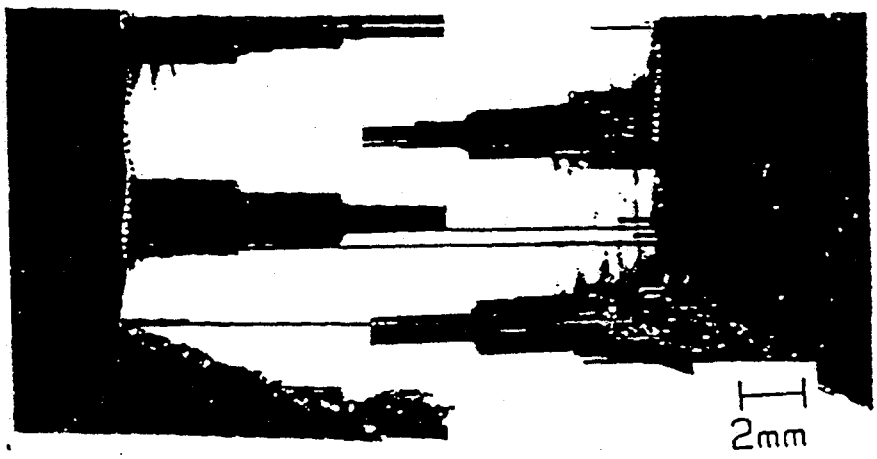

Fig. 10. The fractured joint with the stepped sawtooth geometry showing extreme fiber pullout.

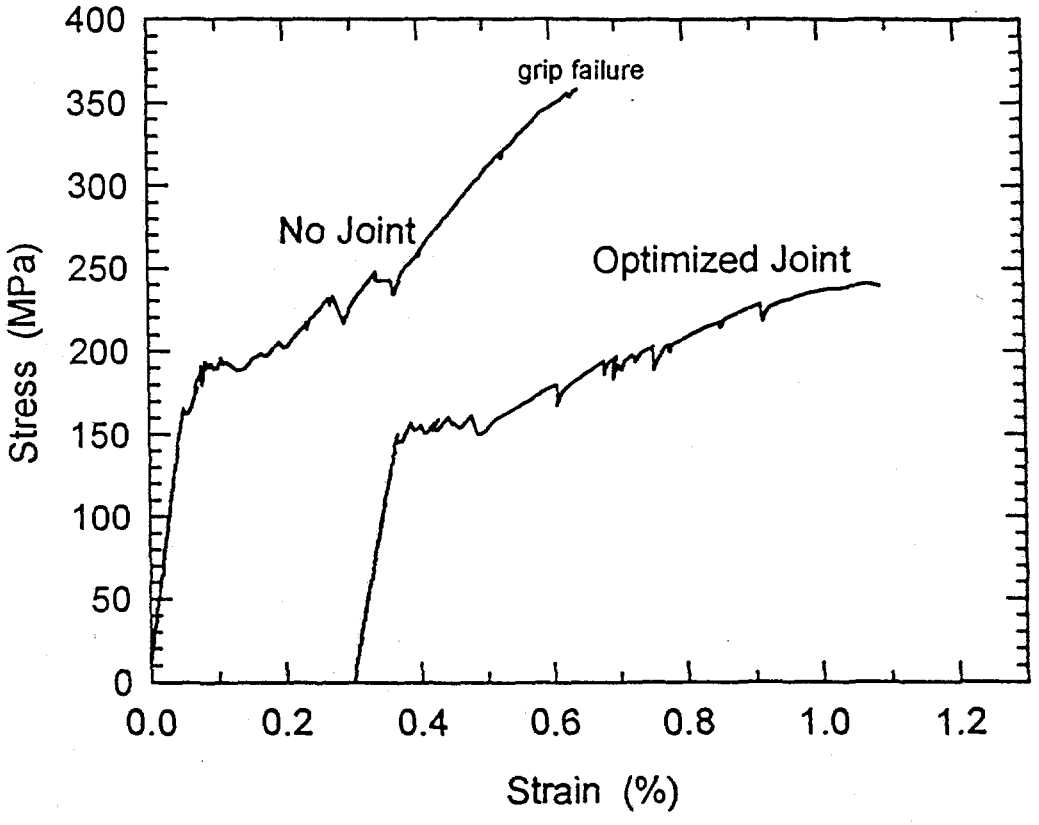

Fig.11 The stress/strain curve for the joint shown in Fig. 8a made with composite with Si_3N_4 fiber coating. The curve for composite not containing a joint is shown for comparison.